Journal of Nano- and Electronic Physics
Vol. **18** No 1, 01027(6pp) (2026)

Журнал нано- та електронної фізики
Том **18** № 1, 01027(6cc) (2026)

OPEN ACCESS

REGULAR ARTICLE

Conditions for Pulse Gas-Discharge Synthesis of Thin Films with High Ion Conductivity

O.K. Shuaibov* ✉, R.V. Hrytsak, O.Y. Minya, Yu.Yu. Bilak, A.O. Malinina, Z.T. Homoki, A.M. Reblian

Uzhhorod National University, 88000 Uzhhorod, Ukraine

(Received 04 October 2025; revised manuscript received 22 February 2026; published online 25 February 2026)

The results of experimental study of the characteristics of high-voltage nanosecond discharge between electrodes of polycrystalline argyrodite (Ag_8GeS_6) in air at different pressures (p = 7-101 kPa) and different frequencies of voltage pulses are presented. The introduction of vapors of the electrode material into the dis-charge plasma occurred as a result of the ectonic mechanism. High spatial uniformity of the discharge was ignited by preliminary ionization of the discharge gap with a beam of runaway electrons and the accompanying soft X-ray radiation. The spatial and spectral characteristics of the discharge were studied at a distance between the electrodes of 2 mm. The optimal conditions for the deposition of thin films based on the superionic conductor Ag_8GeS_6 compound from the discharge plasma onto a solid substrate installed near the electrode system are established. The synthesized thin films may find applications in all-solid-state lithium-ion batteries and supercapacitors.

Keywords: Nanosecond discharge, Argyrodite, Air, Plasma, Emission spectrum, Plasma parameters, Thin films.

DOI: 10.21272/jnep.18(1).01027 PACS numbers: 52.80. − s, 51.50. + v, 52.80.Tn, 52.90. + z, 52.80.Mg, 79.60.Jv

1. INTRODUCTION

All-solid-state lithium batteries with solid electrolytes offer several key benefits for real-world use compared to conventional lithium batteries utilizing liquid electrolytes, particularly in terms of enhanced safety and long-term operational stability [1]. This work critically analyzes the limiting factors of solid-state electrolytes composed of oxides, sulfides, and polymers, including the challenge of improving their ionic transport properties, and outlines both the current challenges and future directions for creating novel types of solid electrolytes.

Lithium-argyrodite solid-state electrolytes are promising for use in high-performance all-solid-state batteries, since they have low cost, exhibit excellent lithium-ion transport properties and favorable electrochemical performance [2]. It also summarizes the latest achievements and limitations of lithium argyrodites for solid-state batteries, which included: synthesis of lithium argyrodites, electrolyte structure, chemical/electrochemical stability, lithium dynamics and battery applications.

In [3], the results of the study of single crystals of $Ag_{7+x}(P_{1-x}Ge_x)S_6$ (x = 0.1, 0.25, 0.33, 0.5, 0.75) of new superionic conductors that had the argyrodite structure are presented. The superionic conductors $Ag_{7+x}(P_{1-x}Ge_x)S_6$ were grown by the method of directed crystallization.

The results of the study of the microstructural, mechanical and electrical characteristics of superionic ceramic materials $Ag_{6+x}(P_{1-x}Ge_x)S_5$ I are presented in [4]. In this case, solid solutions in the form of ceramics were produced using cold pressing of microcrystalline powders.

The synthesized ceramics demonstrated high ionic conductivity, which had a maximum for the composition $Ag_{6,75}(P_{0,25}Ge_{0,75})S_5$ I.

As follows from the works [3, 4], new compounds of the argyrodite type based on silver and germanium are obtained mainly in the form of crystals or ceramics, but for a significant number of their applications in micro-nanoelectronics, thin films with high ionic conductivity are required. It is most expedient to synthesize such films from polycrystalline samples of argyrodite or corresponding ceramics by laser synthesis methods, or by exposing such targets to intense ion or electron beams. However, such technologies require the use of expensive laser and high-vacuum equipment. More economical and promising for practice may be electrical technology based on the explosion of thin conductors or plates. However, such discharge devices operate in a single-use mode and require constant replacement of thin conductors that have transitioned into a plasma state, from which a thin film of the corresponding composition is deposited. In addition, producing thin wires or plates from argyrodite may pose significant challenges. A more promising alternative is pulse-periodic pulsed technology, which relies on the generation of ecton phenomena [5]. In this

* Correspondence e-mail: alexsander.shuaibov@uzhnu.edu.ua

Cite this article as: O.K. Shuaibov, et al., *J. Nano- Electron. Phys.* 18 No 1, 01027 (2026) https://doi.org/10.21272/jnep.18(1).01027

process, microexplosions of natural surface inhomogeneities on the electrode occur under the influence of a strong electric field generated by an overvoltage nanosecond discharge, leading to the injection of electrode material into the plasma. In this manner, thin films derived from $CuInSe_2$, $CuAlInSe_2$ compounds [6, 7], as well as oxide films containing copper, iron, zinc, and aluminum [8-10], have been successfully synthesized.

Currently, the characteristics of nanosecond discharges at atmospheric pressure between argyrodite electrodes remain unexplored, which hampers the practical application of this approach for fabricating argyrodite-based thin films. Therefore, determining the favorable parameters for the introduction of argyrodite vapor into the plasma of a nanosecond discharge and understanding the behavior of such discharges is of great interest.

This article presents an investigation into the spatial, electrical, and spectral properties of overvoltage nanosecond discharges (OND) in an "air – Ag_8GeS_6" gas-vapor mixture, and identifies suitable conditions for the deposition of argyrodite-derived thin films onto a solid substrate positioned near the electrode assembly.

2. METHODOLOGY AND TECHNIQUE OF THE EXPERIMENT

A nanosecond-duration OND was initiated between two electrodes composed of polycrystalline Ag_8GeS_6 material. The electrodes were spaced 2 mm apart, and the radius of curvature at the ends of the cylindrical electrodes was 5 mm.

The setup diagram, design of the discharge system, and experimental conditions for investigating the properties of an overvoltage nanosecond discharge in the "air – Ag_8GeS_6" gas-vapor mixture are detailed in [9].

The discharge was initiated under conditions of overvoltage across the gap, which led to the formation of a beam of runaway electrons [11]. Under the influence of this beam, the discharge in air containing minor amounts of Ag_8GeS_6 vapor impurities at a pressure of 101 kPa remained spatially uniform (Fig. 1) at voltage pulse repetition rates ranging from 80 to 1000 Hz.

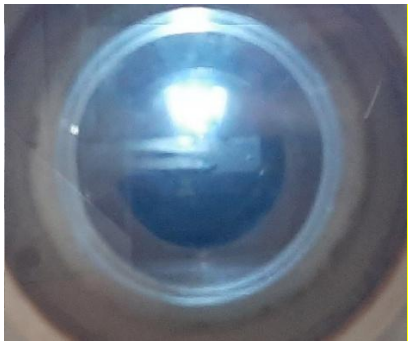

Fig. 1 – Photo of the OND between electrodes of the polycrystalline compound Ag_8GeS_6 in a gas-vapor mixture of "air – Ag_8GeS_6" at a pressure of $p = 101$ kPa and a repetition frequency of voltage pulses of 80 Hz

At $f = 1000$ Hz, the discharge had the largest aperture, which was close to a square with a side of 2 mm. Such a discharge consists of a large number of thin plasma filaments [12], therefore, unlike a conventional spark, they cover the surface of the electrodes quite homogeniuos, which is important for obtaining a sufficient concentration of vapors of the Ag_8GeS_6 compound and uniform evaporation of the working surface of the electrodes.

In a strong electric field between polycrystalline electrodes, microexplosions of natural inhomogeneities of the electrode surface and the formation of ectons occur on their working surfaces [5]. As a result of these processes, vapors of the Ag_8GeS_6 compound were introduced into the discharge plasma. In the plasma, the processes of dissociation of the Ag_8GeS_6 compound and excitation and ionization of its fragments occur, from which a flow of clusters and nanoparticles based on the Ag_8GeS_6 compound was formed. The latter were deposited outside the plasma on a solid glass substrate in the form of thin films.

The surface of the samples of the films synthesized in this way was examined using an optical microscope with a magnification of 500 times.

Polycrystalline samples of Ag_8GeS_6 compounds, which are superionic conductors, were synthesized in the technological laboratory of the State Higher Educational Institution "Uzhhorod National University".

3. DISCHARGE PARAMETERS AND RESULTING MICROSTRUCTURES

The voltage pulse applied between the electrodes in atmospheric-pressure air exhibited damped temporal oscillations lasting approximately 10-20 ns due to the impedance mismatch between the high-voltage modulator and the dynamic resistance of the plasma. The total duration of the pulse sequence reached 450 ns. A pulse transformer with a gain factor of 4 was employed in the high-voltage pulse modulator capable of generating both positive and negative polarity pulses.

At a charging voltage of 21 kV applied to the storage capacitor of the high-voltage system, and under discharge conditions in atmospheric air, the peak voltage drop across the electrodes occurred at the initial stage of the discharge and reached approximately ± 12-17 kV, with a current of about ± 120 A and peak pulse power of 1.0 MW. This provided an energy input of roughly 52 mJ per discharge pulse to the plasma.

The spectrum of plasma radiation in the gas-vapor mixture "air – Ag_8GeS_6" at atmospheric air pressure and a distance between the electrodes of 2 mm is shown in Fig. 2. The results of the identification of spectral lines in this spectrum are given in Table 1. The reference book [13] was used to decipher the spectrum.

In the bactericidal wavelength range (200-280 nm; Table 1), the primary radiation originated from transitions of the singly charged silver ion.

The strongest emission was observed at the Ag II lines of 232.02 and 233.13 nm. This spectral region

closely resembled the equivalent segment of the emission spectrum observed in plasma from an overvoltage discharge between polycrystalline silver sulfide (Ag_2S) electrodes [14, 15], but with greater spectral line density and higher intensity of Ag II radiation in the argyrodite plasma. Among the atomic silver lines, the most intense were those at 328.06 and 338.28 nm (Ag I), corresponding to transitions from the ground state of the silver atom.

Germanium in the plasma emission spectrum was represented by a rather intense spectral atomic line 303.90 nm Ge I and an ion line 607.83 nm 607.83. At atmospheric pressure of air, characteristic emission bands of nitrogen molecules in the spectral range 280-390 nm were not detected, which is typical for plasma of a spark nanosecond discharge at atmospheric pressure [16, 17].

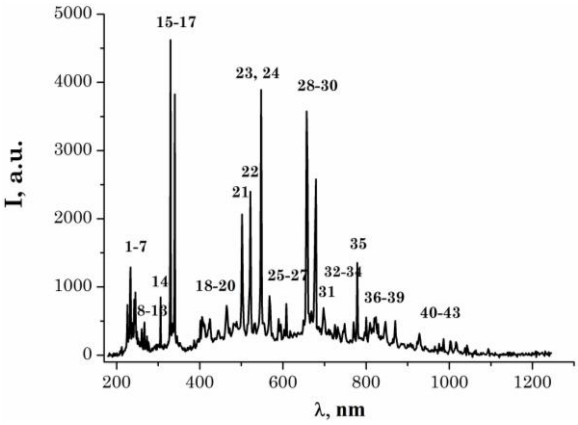

Fig. 2 – Optical emission spectrum of the plasma formed during an overstressed nanosecond discharge between electrodes made of Ag_8GeS_6 at atmospheric pressure (p = 101 kPa) and a repetition rate of 1000 Hz

The most intense ion spectral line of nitrogen was the 500.5 nm N II line. As for a nanosecond spark discharge in air at atmospheric pressure, plasma emission on transitions of a single-atom oxygen atom was concentrated in the near infrared region of the spectrum (700-975 nm; Table 1).

The highest intensity was the 777.19 nm O I line. Sulfur radiation in the plasma was represented only by lines of the sulfur atom in the spectral range 870-965 nm, of which the highest radiation intensity was the line with a wavelength of 869.47 nm S I.

This pattern of intensity distribution in the emission spectrum results from the pulsed nature of the current. Consequently, stepwise processes take place within the plasma, including dissociative excitation and dissociative ionization of Ag_8GeS_6 molecules. Following the generation of plasma ions, recombination processes commence, leading to the population of excited states of the primary plasma species: Ag I, Ag II, Ge I, Ge II, N II, and O I.

Tables 2 and 3 show the dependences of the intensity of ultraviolet spectral lines of argyrodite plasma on air pressure at a fixed frequency and frequency at a fixed air pressure.

When the air pressure decreased from 101 to 7 kPa, a significant decrease in the radiation intensity was observed for all spectral lines of silver and germanium atoms, as well as the silver ion, which could exceed one order of magnitude.

This is due to a decrease in the energy contribution to the plasma at low air pressures and a decrease in the efficiency of ecton formation, which determines the density of argyrodite vapors in the plasma. The characteristic UV bands of the nitrogen molecule – N2(A-C) were recorded only at low air pressures, which are characterized by the diffuse stage of the nanosecond discharge. With increasing air pressure, the intensity of these bands decreased to zero and only the spectral bands of the atomic nitrogen ion were recorded in the spectrum, which is characteristic of an overvoltage nanosecond discharge and a nanosecond spark discharge in air at atmospheric pressure. The intensity of such a line with a wavelength of 333.13 nm N II increased with air pressure (Table 2).

Increasing the repetition rate of voltage pulses from 35 to 1000 Hz at $p_{(air)}$ = 7 kPa resulted in a significant rise in the intensity of all UV emission lines. A similar trend was observed with frequency growth at atmospheric pressure (101 kPa). This behavior is primarily explained by a higher concentration of argyrodite vapors in the plasma caused by an increase in the average discharge power.

Thus, the optimal conditions for the deposition of thin films based on argyrodite from a nanosecond discharge plasma are realized at a frequency of 1000 Hz and an air pressure of 101 kPa. This is important for the development of an open (windowless) plasma chemical reactor for the synthesis of thin films of argyrodite which can operate with a free buffer gas without the use of vacuum technology.

When a glass substrate was positioned 2-3 cm away from the center of the discharge gap and the discharge was maintained for 30-40 minutes, a thin film formed on the substrate as a result of electrode material sputtering in air. The typical size of the surface features within the deposited film was 10-20 μm (Fig. 3), and the overall film area ranged from 1 to 1.5 cm^2.

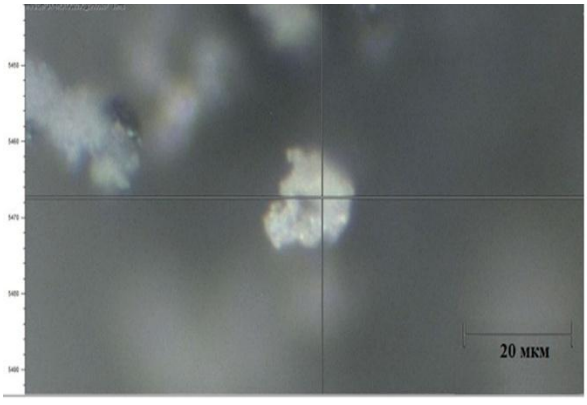

Fig. 3 – Photo of the surface of the synthesized argyrodite film deposited from the plasma of an overvoltage nanosecond discharge between argyrodite electrodes at atmospheric air pressure

Table 1 – Spectral line identification results for the plasma generated by discharge between Ag_8GeS_6 electrodes, corresponding to Fig. 2

No	λ_{tab}, nm	I_{exp} a.u.	Object	E_{low}, eV	E_{up}, eV	Lower term	Upper term
1	224.64	738	Ag II	4.85	10.37	$4d^9(^2D_{5/2})5s\ ^2[5/2]_3$	$4d^9(^2D_{5/2})5p\ ^2[7/2]^\circ_4$
2	227.99	361	Ag II	5.70	11.14	$4d^9(^2D_{3/2})5s\ ^2[^3/_2]_2$	$4d^9(^2D_{3/2})5p\ ^2[^3/_2]^\circ_1$
3	232.02	1059	Ag II	5.70	11.05	$4d^9(^2D_{3/2})5s\ ^2[^3/_2]_2$	$4d^9(^2D_{3/2})5p\ ^2[^5/_2]^\circ_3$
4	233.13	1287	Ag II	5.05	10.36	$4d9(^2D_{5/2})\ 5s^2[5/2]_2$	$4d^9(^2D_{5/2})\ 5p\ ^2[3/2]^\circ_1$
5	241.13	815	Ag II	5.42	10.56	$4d^9(^2D_{3/2})5s\ \ ^2[^3/_2]_1$	$4d^9(^2D_{5/2})5p\ \ ^2[^5/_2]^\circ 2$
6	243.77	619	Ag II	4.85	9.94	$4d^9(^2D_{5/2})5s\ ^2[5/2]_3$	$4d^9(^2D_{5/2})5p\ ^2[3/2]^\circ_2$
7	244.78	919	Ag II	5.70	10.77	$4d^9(^2D_{3/2})5s\ ^2[^3/_2]_2$	$4d^9(^2D_{3/2})5p\ \ ^2[^5/_2]^\circ 2$
8	260.59	382	Ag II	10.18	14.94	$4d^9(^2D_{5/2})\ 5p\ \ ^2[^7/_2]^\circ_3$	$4d^9(^2D_{5/2})6s\ ^2[^5/_2]_3$
9	261.43	121	Ag II	10.77	15.51	$4d^9(^2D_{3/2})5p\ ^2[^5/_2]^\circ_2$	$4d^9(^2D_{3/2})6s\ ^2[^3/_2]_1$
10	266.04	481	Ag II	12.14	16.78	$4d^85s^2\ \ ^3F_3$	$4d^8(^3F)5s5p(^3P^\circ)^5G^\circ_2$
11	271.17	278	Ag II	10.37	14.94	$4d^9(^2D_{5/2})\ 5p\ ^2[^7/_2]^\circ_4$	$4d^9(^2D_{5/2})\ 6s\ 2[^5/_2]\ 3$
12	276.75	191	Ag II	5.70	10.18	$4d^9(^2D_{3/2})5s\ ^2[^3/_2]_2$	$4d^9(^2D_{5/2})5p\ ^2[^7/_2]^\circ_3$
13	293.83	153	Ag II	10.77	14.99	$4d^9(^2D_{3/2})5p\ ^2[^5/_2]^\circ_2$	$4d^9(^2D_{5/2})6s\ ^2[^5/_2]_2$
14	303.90	848	Ge I	0.88	4.96	$4s^24p^2\ ^1D_2$	$4s^24p5s\ \ ^1P^\circ_{3/2}$
15	328.06	4619	Ag I	0.00	3.77	$4d^{10}5s\ ^2S_{1/2}$	$4d^{10}5p\ ^2P^\circ_{3/2}$
16	333.13	467	N II	20.65	24.37	$2s^22p3p\ ^3D_2$	$2s^22p4s\ ^3P^\circ_1$
17	338.28	3822	Ag I	0.00	3.66	$4d^{10}5s\ ^2S_{1/2}$	$4d^{10}5p\ ^2P^\circ\ _{1/2}$
18	405.54	561	Ag I	3.66	6.72	$4d^{10}5p\ ^2P^\circ\ ^1/_2$	$4d^{10}6d\ ^2D_{3/2}$
19	424.06	530	Ag II	14.08	17.00	$4d^85s^2\ \ ^1G_4$	$4d^9(^2D_{3/2})6p\ \ ^2[^5/_2]^\circ_3$
20	464.30	724	N II	18.47	21.15	$3s\ ^3P^0$	$3p\ ^3P$
21	500.515	2064	N II	20.66	23.14	$2s^22p3p\ \ ^3D_3$	$2s^22p3d\ ^3F^\circ_4$
22	520.90	2397	Ag I	3.66	6.04	$4d^{10}5p\ ^2P^\circ_{1/2}$	$4d^{10}5d\ ^2D_{3/2}$
23	531.24	470	Ag II	15.70	18.03	$4d^9(^2D_{5/2})5d\ ^2[^9/_2]_4$	$4d^9(^2D_{5/2})\ 4f\ \ ^2[^9/_2]^\circ_4$
24	547.86	3889	Ag II	15.71	17.97	$4d^9(^2D_{5/2})5d\ ^2[^3/_2]2$	$4d^9(^2D_{5/2})4f\ ^2[^1/_2]^\circ_1$
25	566.66	867	N II	18.46	20.65	$2s^22p3s\ \ ^3P^\circ_1$	$2s^22p3p\ \ \ ^3D_2$
26	594.16	452	N II	21.16	23.24	$3p\ ^3P_2$	$3d\ ^3D^0_3$
27	607.83	751	Ge II	15.46	17.50	$4s4p(^3P^\circ)\ 5s\ \ ^4P^\circ{}^5/_2$	$4s4p(^3P^\circ)\ 5p\ \ ^4D^7/_2$
28	657.07 - second order 328.06	3573	Ag I	0.00	3.77	$4d^{10}5s\ ^2S_{1/2}$	$4d^{10}5p\ ^2P^\circ_{3/2}$
29	668.3 - second order 333.13	642	N II	20.65	24.37	$2s^22p3p$ $^3D_2$	$2s^22p4s$ $^3P^\circ_1$
30	679.2 - second order 338.28	2578	Ag I	0.00	3.66	$4d^{10}5s\ ^2S_{1/2}$	$4d^{10}5p\ ^2P^\circ\ _{1/2}$
31	700.22	587	O I	10.99	12.76	$3p\ ^3P_2$	$4d\ ^3D^0_1$
32	711.00	379	O II	29.06	30.81	$2s^22p^2(^3P)3d\ ^2D_{5/2}$	$2s^22p^2(^3P)4p\ \ \ ^2P^\circ_{3/2}$
33	725.44	445	O I	10.99	12.70	$3p\ ^3P$	$5s\ ^3S_0$
34	770.67	484	O I	14.05	15.65	$3p'\ ^3D_{2,3}$	$2p^5\ ^3P^0_2$
35	777.19	1354	O I	9.14	10.74	$3s\ ^5S^02$	$3p\ ^5P_3$
36	800.51	554	Ag II	14.94	16.49	$4d^9(^2D_{5/2})6s\ ^2[^5/_2]_3$	$4d^9(^2D_{5/2})\ 6p\ ^2[^5/_2]^\circ_3$
37	822.47	558	Ag II	14.94	16.45	$4d^9(^2D_{5/2})6s\ _2[5/2]_3$	$4d^8(^3F)5s5p(^3P^\circ)\ ^5G^\circ_4$
38	844.67	429	O I	9.52	10.99	$3s\ ^3S^0_1$	$3p\ ^3P_1$
39	869.47	502	S I	7.86	9.29	$3s^23p^3\ (^4S^\circ)\ 4p\ ^5P_3$	$3s^23p^3(^4S^\circ)4d\ 5D^\circ_4$
40	942.19	129	S I	8.40	9.72	$3s^23p^3(^2D^\circ)4s\ \ ^3D^\circ_2$	$3s^23p^3(^2D^\circ)4p\ \ ^3F_3$
41	964.95	128	S I	8.41	9.69	$3s^23p^3(^2D^\circ)\ 4s\ \ ^3D^\circ_3$	$3s^23p^3(^2D^\circ)\ 4p\ \ ^3D_3$
42	974.149	168	O I	14.13	15.40	$3p'\ ^1F_3$	$3d'\ ^3G^0_4$
43	1002.32	207	N II	26.21	27.45	$4fG(4^1/_2)_5$	$5g\ H(5^1/_2)_{5,6}$

Table 2 – Dependence of the relative intensity of the emission of spectral lines of plasma of an overvoltage nanosecond discharge between electrodes with Ag_8GeS_6 on air pressure at a frequency f = 1000 Hz

No	λ_{tab}, nm	Object	I_{exp} a.u. p = 7 kPa	I_{exp} a.u. p = 21 kPa	I_{exp} a.u. p = 101 kPa
1	224.64	Ag II	140	344	738
2	227.99	Ag II	47	137	361
3	232.02	Ag II	120	315	1059
4	233.13	Ag II	180	489	1287
5	241.13	Ag II	50	270	815
6	243.77	Ag II	63	220	619
7	244.78	Ag II	115	287	919
8	260.59	Ag II	125	140	382
9	261.43	Ag II	44	106	121
10	266.04	Ag II	152	255	481
11	271.17	Ag II	87	112	278
12	276.75	Ag II	77	115	191
13	293.83	Ag II	28	84	153
14	297.68	N_2	156	-	-
15	303.90	Ge I	351	501	848
16	315.93	N_2	347	-	-
17	328.06	Ag I	625	1657	4619
18	333.13	N II	-	137	467
19	338.28	Ag I	1181	1374	3822
20	357.69	N_2	384	-	-

Table 3 – Dependence of the relative intensity of the emission of spectral lines of the plasma of an overvoltage nanosecond discharge between electrodes with Ag_8GeS_6 on the frequency at air pressure p = 7 kPa

№	λ_{tab}, nm	Object	I_{exp} a.u. 35 Hz	I_{exp} a.u. 80 Hz	I_{exp} a.u. 150 Hz	I_{exp} a.u. 250 Hz	I_{exp} a.u. 400 Hz	I_{exp} a.u. 1000 Hz
1	224.64	Ag II	87	51	172	297	872	738
2	227.99	Ag II	30	38	102	109	395	361
3	232.02	Ag II	77	34	133	291	1100	1059
4	233.13	Ag II	111	85	216	415	1329	1287
5	241.13	Ag II	50	22	132	213	821	815
6	243.77	Ag II	53	40	113	170	647	619
7	244.78	Ag II	80	52	170	112	886	919
8	260.59	Ag II	38	24	112	89	421	382
9	261.43	Ag II	58	39	100	50	211	121
10	266.04	Ag II	53	15	92	104	232	481
11	271.17	Ag II	39	27	69	65	323	278
12	276.75	Ag II	28	19	70	64	232	191
13	293.83	Ag II	58	43	117	43	127	153
14	303.90	Ge I	55	61	150	127	899	848
15	328.06	Ag I	207	274	565	908	3779	4619
16	333.13	N II	65	102	271	72	253	467
17	338.28	Ag I	173	223	484	722	3077	3822
18	405.54	Ag I	111	129	391	111	246	561
19	424.06	Ag II	85	113	330	107	342	530
20	464.30	N II	131	196	455	143	313	724

4. CONCLUSIONS

Experimental studies of the overvoltage nanosecond discharge (OND) in air between electrodes composed of Ag_8GeS_6 have shown:

– the discharge plasma emitted UV radiation corresponding to transitions of neutral silver atoms and singly charged silver ions; the resonant spectral lines of the silver atom (328.06 and 338.28 nm Ag I) stood out due to their high intensity;

– the maximum UV emission intensity from silver atoms and singly charged ions was recorded at an air pressure of 101 kPa, with the working capacitor of the high-voltage pulse modulator charged to its highest voltage and operating at a repetition frequency of 1000 Hz, which corresponded to the optimal conditions for synthesizing argyrodite-based thin films;

– during the deposition of electrode erosion products

from the plasma onto a glass substrate placed near the electrode system, thin films based on argyrodite with an area of approximately 1-1.5 cm^2 were successfully synthesized;

– the OND generated between argyrodite electrodes in air can serve as a source of synchronized UV radiation and micro- to nanoparticles derived from the Ag_8GeS_6 compound, which have potential applications in medicine and microbiology due to their strong antimicrobial effects.

REFERENCES

1. Z. Wu, Z. Xie, A. Yoshida, Z. Wang, X. Hao, A. Abudula, G. Guan, *Renew. Sustain. Energy Rev.* **109**, 367 (2019).
2. C. Yu, F. Zhao, J. Luo, L. Zhang, X. Sun, *Nano Energy* **83**, 105858 (2021).
3. A.I. Pogodin, M.J. Filep, V.I. Studenyak, O.I. Symkanych, I.P. Stercho., V.Yu. Izai, O.P. Kokhan, P. Kúš, *J. Alloy. Compd.* **926**, 166873 (2022).
4. A.I. Pogodin., M.J. Filep, T.O. Malakhovska, V.V. Vakulchak, V. Komanicky, V.Yu. Izai, Y.I. Studenyak, Y.P. Zhukova, I.O. Shender, V.S. Bilanych, O.P. Kokhan, P. Kúš, *J. Phys. Chem. Solids* **171**, 111042 (2022)
5. G.A. Mesyac, M.I. Yalandin, *Phys.-Usp.* **189** No 7, 747 (2014).
6. A.K. Shuaibov, A.Y. Minya, R.V. Hrytsak, A.A. Malinina, A.N. Malinin, *Advances in Nanoscience and Nanotechnology* **4** No 1 (2020).
7. A.K. Shuaibov, A.I. Minya, A.A. Malinina, R.V. Gritsak, A.N. Malinina, Yu.Yu. Bilak, M.I. Vatrala, *Surface Engineering and Applied Electrochemistry* **58** No 4, 370 (2022).
8. O.K. Shuaibov, A.O. Malinina, *Progr. Phys. Metals* **22** No 3, 382 (2021).
9. O.K. Shuaibov, O.Y. Minya, A.O. Malinina, O.M. Malinin, I.V. Shevera, *Nanosistemi, Nanomateriali, Nanotehnologii*, **19** No 1, 189 (2021).
10. A. Shuaibov, A. Malinina, A. Malinin, *Overstressed nanosecond discharge in gases at atmospheric pressure and its application for the synthesis of nanostructures based on transition metals* (Beau Bassin: Lap. Lambert Academic Publishing.: 2021).
11. *Runaway electrons preionized diffuse discharge* (Ed. by V.F. Tarasenko) (New York: Nova Science Publishers Inc.: 2014).
12. A.A. Trenkin, K.I. Almazova, A.N. Belonogov, V.V. Borovkov, A.S. Dolotov, I.V. Morozov, *Tech. Phys.* **69** No 2, 431 (2024).
13. NIST Atomic Spectra Database Lines Form.
14. O.K. Shuaibov, R.V. Hrytsak, R.P. Romanets, *The III International Scientific and Practical Conference – Modern challenges to science and practice*, 483 (Varna:2022).
15. A. Shuaibov, A. Minya, R. Hrytsak, A. Malinina, A. Malinin, Yu. Zhiguts, I. Shevera, *Biomed. Translat. Sci.* **2** No 1, 1 (2022).
16. R.M. van der Horst, T. Verreycken, E.M. van Veldhuizen, P.J. Bruggerman, *J.Phys. D: Appl. Phys.* **45**, 345201 (2012).
17. J.M. Palomares, A. Kohut, G. Galbacs, R. Engeln, Zs. Geretovszky, *J. Appl. Phys.* **118**, 233305 (2015).

Умови імпульсного газорозрядного синтезу тонких плівок з високою іонною провідністю

О.К. Шуаібов Р.В. Грицак, О.Й. Миня, Ю.Ю. Білак, А.О. Малініна, З.Т. Гомокі, А.М. Реблян

ДВНЗ «Ужгородський національний університет», 88000 Ужгород, Україна

Наведено результати експериментального вивчення характеристик високовольтного наносекундного розряду між електродами з полікристалічного аргіродиту (Ag_8GeS_6) в повітрі при різних тисках (p = 7 – 101 кПа) та різних частотах слідування імпульсів напруги. Внесення парів матеріалу електродів в плазму розряду відбувалось в результаті ектонного механізму. Висока просторова однорідність розряду забезпечувалась попередньою іонізацією розрядного проміжку пучком електронів – втікачів і супутнього йому м'якого рентгенівського випромінювання. Досліджено просторові і спектральні характери-стики розряду при віддалі між електродами – 2 мм. Встановлено оптимальні умови осадження з плазми розряду на тверду підкладку, встановлену біля системи електродів, тонких плівок на основі суперіонного провідника – сполуки Ag_8GeS_6. Синтезовані тонкі плівки можуть знайти застосування в повністю твердотільних літій-іонних батареях і суперконденсаторах.

Ключові слова: Наносекундний розряд, Аргіродит, Повітря, Плазма, Спектр випромінювання, Параметри плазми, Тонкі плівки.